

Strain measuring accuracy with splitting-beam laser extensometer technique at split Hopkinson compression bar experiment

R. PANOWICZ*, J. JANISZEWSKI, and M. TRACZYK

Military University of Technology, 2 Gen. Kaliskiego Str., 00-908 Warsaw, Poland

Abstract. An accuracy problem of strain measurement at compression split Hopkinson compression bar experiments with a splitting-beam laser extensometer was considered. The splitting-beam laser extensometer technique was developed by Nie et al. to measure strain of a specimen during its tension under a high strain rate loading condition. This novel concept was an inspiration for the authors to develop own laser extensometer system, which allows for simultaneous and independent measurement of displacement of bar ends between which a compressed material specimen is placed. In order to assess a metrological property of this measuring system, a wide range of high strain rate experiments were performed, including tests with various sample materials (Al 5251, Cu OFE) with different rate of strain, and with the use of two bars material. A high accuracy of the developed laser extensometer was found in measurement of specimen strain, for which uncertainty is not greater than 0.1% and, for a typical specimen dimension, the maximum permissible error is 4.5 μm .

Key words: SHPB test, strain rates, non-contact strain measurement, laser extensometer.

1. Introduction

A common practice in split Hopkinson pressure bar (SHPB) experiments and Kolsky bar experiments is to use a reflected pulse to calculate the specimen strain [1]. However, in many cases, the reflected pulse may not be reliable due to complex effects arising from loading dynamics and contact conditions between the specimen and the bars [2]. For example, when the compression SHPB is used to perform dynamic experiments on specimens made of high strength materials with a diameter much smaller than the bar diameter, the assumption of a planar wave in the bars may be violated because of elastic indentation of the specimen into the bar ends (punching effect) [3, 4]. It may result in a significant error in the strain measurements of the specimen, particularly when specimen strain is small. In order to limit the punching effect, high stiffness and high strength platens are placed between the bars and the specimen [5]. However, the introduction of the platens may cause wave disturbances resulting from a wave impedance mismatch and imperfections of the contact surfaces (e.g. parallelism, flatness). Similar problems occur in tensile SHPB, where the stress wave is disturbed at the interfaces of adapters, couplers as well as threads [6, 7]. Moreover, deformation non-uniformity of the specimen gauge section is an additional source of errors in strain measuring in high strain rate tension tests [8, 9]. Therefore, in the SHPB experiments, the strain measurements pose a great challenge and require an advanced measuring technique, particularly while determining the stress-strain response of materials at small strains. Non-contact measuring methods are an alternative for the conventional specimen strain calculation with the reflected pulse.

The simplest approach is to use a high speed digital camera to photograph the specimen deformation [10, 11]. The camera is focused on the entire gauge section and part of the non-gauge section at both ends to achieve a sufficient image with the highest resolution possible. Due to motion analysis of the selected characteristic points, defining the strain gage length, a strain-time relationship can be determined. However, due to the limited frame rate and its corresponding resolution of a contemporary high speed camera, the obtained results did not provide sufficient data points to construct a full stress-strain curve [8].

The high-rate digital image correlation (DIC) is a further development of the above described techniques [12, 13]. In this case, information about specimen deformation is given by motion analysis of a large number of points (speckle) spreading over the surface of the specimen gauge length [14, 15]. A random speckle pattern is generated by a spraying black paint and a white base layer directly onto the surface of the specimen. Thus, DIC provides highly valuable information on dynamic full-field strain measurements in the specimen, however, the above-mentioned limitations resulting from the usage of a contemporary high speed camera and an extreme difficulty in acquiring a large quantity of high-resolution images at very high frame rates do not allow for constructing a precise stress-strain curve [8].

Another strain measuring technique is the interferometric-strain-gauge method, which is one of the first diagnostic techniques applied to straightforward non-contact measurement of specimen strain in SHPB testing. Sharpe et al. [16] used this method for evaluation of strain uniformity in the compressed specimen by comparison of surface strain at the specimen midpoint to the average strain calculated from the conventional Kolsky bar analysis. They found that the midpoint strain and the average strain agree quite well. Recently, Casem et al. have

*e-mail: robert.panowicz@wat.edu.pl

applied an interferometric technique to measure the displacement of the incident and transmitted bars in the small diameter SHPB arrangement, which allowed investigating Al 6061-T6 alloy with a very high strain rate (order of 10^5 1/s) [17, 18].

Another non-contact method used for measuring strain is the laser extensometer. It consists of three major components: optical system for generating a laser sheet, optoelectronics system for collecting the light, and mounting systems. The basic principle of operation of this measuring system is relatively simple. When a specimen is deformed, the change in dimensions of a specimen or a gap between front bars surfaces causes the change in amount of the light collected by the detector located behind the specimen. Thus, by recording the output of the photodiode during the test and using calibration data (relationship between the voltage output and dimensions of the specimen), deformations of the specimen during the SHPB experiment are obtained. Ramesh and Narasimhan applied this technique for measuring radial strain of a specimen compressed under SHPB loading condition with the use of a measuring system called laser occlusive radius detector (LORD) [19]. This approach was also applied to a tension SHPB experiment, with satisfactory results, by Li et al. [20], who studied the dynamic tensile behavior of several metallic alloys and composites. However, a slight variation in laser intensity along the measurement gauge section may induce a significant error, particularly in the case of tests at small strains. Recently, therefore, Nie et al. [21] have proposed a novel measuring technique called splitting-beam laser extensometer, which allowed for measuring the motions of the incident and transmission bar ends independently, thus offering better chances to improve the accuracy of strain determination. This innovative measuring idea was an inspiration for the authors to develop their own measuring system, based on which the accuracy problem of specimen strain measurement with a splitting-beam laser extensometer technique in compression SHPB experiments was considered.

The paper is organized as follows: Section 2 is devoted to the description of the used SHPB arrangement and experimental conditions. The design and operation of a splitting-beam laser extensometer and an analysis of factors affecting its measuring accuracy are presented in Section 3. A description of experimental investigations verifying the accuracy of the tested measuring system under different conditions of SHPB experiments and discussion on the obtained results are included in Section 4.

2. Experimental set-up

The dynamic tests were performed using the classical split Hopkinson compression bar technique (Fig. 1). The basic parameters of the system are as follows: input and output bar length – 1200 mm, striker bar length – 250 mm, all the bars diameter – 12 mm. The striker bar was driven by a compressed air system with a barrel length and diameter equal to 1200 mm and 12.1 mm, respectively. The velocities applied during the experiment were in the range of 6 to 12 m/s. In order to limit Pochhammer-Chree oscillations, a pulse wave technique was applied (copper disk – 3 mm in diameter and 0.2 mm in height)

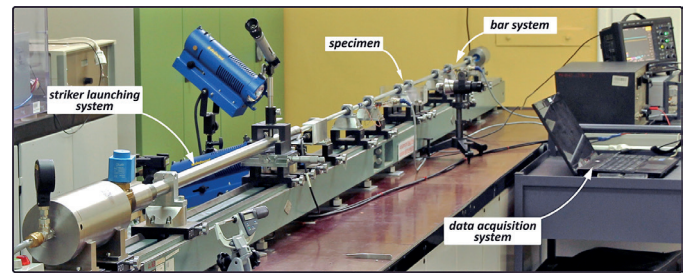


Fig. 1. View of the arrangement used for classical split Hopkinson compression bar

[22, 23]. The plastic flow stress of the sample material was determined according to the classical Kolsky theory (based on the transmitted wave pulse). In turn, the strain and a strain rate were determined on the basis of the reflected signal recorded by the strain gauge glued on the input bar as well as by an optical extensometer. A detailed description of the non-contact measurement system is presented in Section 3.

The measurement system consisted of an amplifier strain gauge SGA-0B V5 Wheatstone bridge with signal conditioning amplifiers, ESA Messtechnik characterized by a high cut-off frequency of 1 MHz and LeCroy WJ354A high-speed digital oscilloscope was used to register the waves signals propagating through the bars. The SHPB system was carefully aligned and calibrated to obtain high quality measurement pulses of the waves. In Fig. 2, the example of raw oscilloscope signals showing smooth and undisturbed wave profiles is presented.

In order to provide a comprehensive assessment of the metrological characteristics of the optical extensometer, the dynamic tests carried out under different experimental conditions, i.e., for two kinds of materials used for the bars and two kinds of materials used for the samples. Aluminum alloy Al 7075-T6 (sound wave velocity – 5170 m/s) bars and maraging steel grade MS350 (sound wave velocity – 4866 m/s) bars were employed

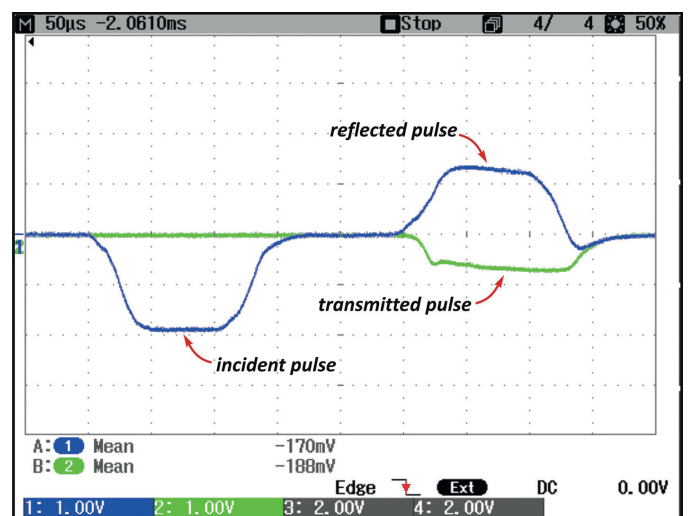


Fig. 2. The raw waves signals measured by the strain gages for aluminum specimen

in the experiments. The verifying tests were performed for two types of the materials, used for samples, with different strength and density: 5251 aluminum as-received and OFE copper as-received. Samples made of Al 5251 were tested on SHPB with aluminum alloy bars due to their low impedance.

The dimensions of the cylindrical samples were as follows: diameter – 5 mm, height – 5 mm. Four tests were carried out for each material of the sample. The dimensions of the samples were measured by means of micrometers with measurement uncertainty equal $\pm 3 \mu\text{m}$.

3. Laser extensometer – accuracy analysis

Based on the concept of an optical extensometer described in [21, 24], the system for measuring the displacements of bars' ends is shown in Fig. 3.

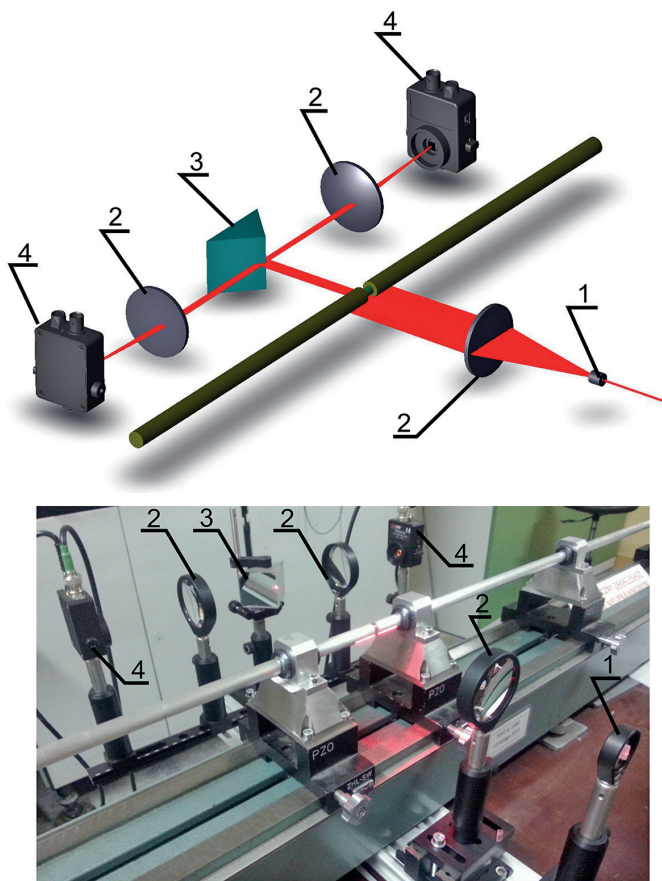


Fig. 3. The scheme of the laser extensometer and the arrangement; 1 – Powell lens, 2 – plano-convex spherical lens, 3 – knife edge right angle prism mirror, 4 – detectors

In this system, a 5 mW He-Ne laser was used for generating coherent light, the power of which varies by less than 2.5% within 8 hours of operation. He-Ne laser generates light with higher stability as compared to the semiconductor laser both in terms of light power as well as its length.

The He-Ne laser beam is formed with Powell lens into a thin line with a uniform intensity distribution and then collimated by plano-convex spherical lens. The light passes through the gap between the incident and the transmitted bar, where the sample is placed. Next, the laser beam is divided in two independent sub-beams using a knife edge right angle prism mirror. The light power in each sub-beam is associated with the current instantaneous position of the bars' ends on which the light impinges. The individual sub-beams are then focused on the detectors recording a change in the light intensity.

Low-noise Thorlabs PDA36A detectors and Aligent DSO7034B oscilloscope were used to collect the signals and store the measured data. The Thorlabs detectors work with bandwidth equal to 1 MHz. It should be noted that this bandwidth is sufficient and recommended for the split Hopkinson compression bar experiments [1, 25]. Detectors worked with 20 dB gain and typical noise ratio equal 0.25 mV.

The voltage value measured by oscilloscope is dependent on the current position of the bar end. It can be expressed with the following equation [26]:

$$U = tg \cdot R(\lambda) \cdot \frac{R_{load}}{R_{load} + R_s} \cdot I, \quad (1)$$

where: tg [V/A] – transimpedance gain, $R(\lambda)$ [A/W] – detector responsivity, R_{load} – load resistance, R_s – detector resistance, I [W] – input light power.

Examples of voltage at the output of the detectors are shown in Fig. 4.

On the other hand, a change of the position of the bar end on which the light impinges can be expressed, using (1), in the following form:

$$\Delta I = a \cdot \Delta U = a \cdot tg \cdot R(\lambda) \cdot \frac{R_{load}}{R_{load} + R_s} \cdot \Delta I, \quad (2)$$

where: a – slope of the calibration line, ΔI – change of light intensity.



Fig. 4. Raw waves signals measured by the laser extensometer, input bar, brown – Detector 1, output bar, green – Detector 2

However, the strain of the sample, which is placed between the bars ends on which the light impinges, can be calculated according to the following relation:

$$\varepsilon = \frac{\Delta l_{in} - \Delta l_{out}}{l_s}, \quad (3a)$$

$$\varepsilon = [(a \cdot \Delta U)_{in} - (a \cdot \Delta U)_{out}] \frac{1}{l_s}, \quad (3b)$$

$$\varepsilon = \left[\left(a \cdot tg \cdot R(\lambda) \cdot \frac{R_{load}}{R_{load} + R_s} \cdot \Delta I \right)_{in} - \left(a \cdot tg \cdot R(\lambda) \cdot \frac{R_{load}}{R_{load} + R_s} \cdot \Delta I \right)_{out} \right] \frac{1}{l_s}, \quad (3c)$$

where: ε – strain, l_s – sample thickness, Δl_{in} – displacement of the input bar end, Δl_{out} – displacement of the output bar end, the index *in* refers to the detector track related to the input bar, and *out* – to the one related to the output bar.

The key issue for high accuracy determination of the sample strain is to precisely carry out the calibration process resulting in determination of the parameter a , occurring in the formula (3c).

The calibration process of the optical extensometer was performed using the gauge blocks. It consisted in placing a selected gauge block between the faces of the lightening bars and reading out the voltage value from the oscilloscope. The gauge blocks with increasing thickness of 0.1 mm in the range of 1 to 2.5 mm were used. The results of the calibration process for both detectors are shown in Fig. 5. It was found that for both detectors (Detector 1, Detector 2) displacement – voltage lines (calibration lines) are characterized by a linear relation (Fig. 5a). A coefficient of multiple correlation R^2 in both calibration lines was equal to 0.9998 and measurement uncertainty was equal to 5.99 $\mu\text{m}/\text{V}$ and 7.29 $\mu\text{m}/\text{V}$ for Detector 1 and 2, respectively. The calculated coefficients of the calibration lines slope were 1.7329 mm/V and 1.7352 mm/V, respectively.

Additionally, some calibration curves for five different positions of the gap(s) relative to the laser sheet shifted in the increment of 0.5 mm are presented in Fig. 5b.

A comparison of normalized calibration lines shows their high parallelism, which proves that distribution of radiation power in the laser sheet is characterized by high uniformity.

Generally, the uncertainty of measurement displacement of the bars ends is not only dependent on uneven distribution of power in the laser beam after passing through the Powell lens [21], but also on electrical noise of signals, fluctuations in a signal power laser source and external lighting conditions during tests. The level of electrical noise observed during the tests was low and equal on average to 0.1063 mV. In turn, an influence of fluctuations of a power laser source on the uncertainty of the specimen strain determination was estimated using the following formula:

$$\delta\varepsilon = |(a \cdot tg \cdot I)_{in} - (a \cdot tg \cdot I)_{out}| \cdot \frac{R(\lambda)}{l_s} \frac{R_{load}}{R_{load} + R_s} \left| \frac{\delta I}{I} \right|, \quad (4)$$

where: $I = I_{in} + I_{out}$, I_{in} – power of the laser beam incident on the Detector 1 and I_{out} – on Detector 2, δI – change of the light intensity, also called a power drift, generated by the He-Ne laser.

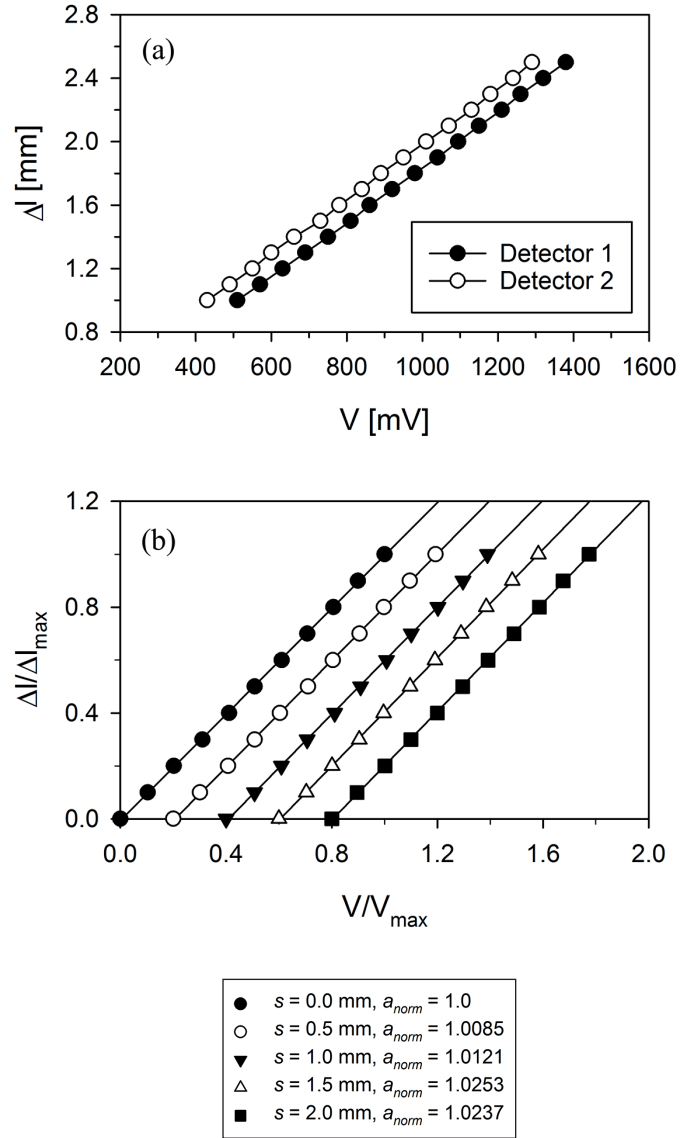


Fig. 5. Calibration lines: a) for Detectors 1 and 2; b) normalized calibration lines for Detector 1 vs. horizontal position s . The lines were shifted in the increment of 0.2 for ease of comparison

Assuming that the product of the gain and light intensity is constant for both detectors, relationship (4) is simplified to the form:

$$\delta\varepsilon = |a_{in} - a_{out}| \cdot tg_{in} I_{in} \frac{R(\lambda)}{l_s} \frac{R_{load}}{R_{load} + R_s} \left| \frac{\delta I}{I} \right|. \quad (5)$$

The uncertainty of strain measurement determined on equation (5) shall not be greater than 14 $\mu\text{m}/\mu\text{m}$. It has been determined for the maximum drift of mean power, which in the case of the used gas laser is not higher than 2.5% after 8 hours of work [26]. In the actual experiment, the overall average duration of 2–3 hours should be 2 to 5 times shorter. In addition, the effect of fluctuation can be minimized by performing additional calibrations carried out before each series of tests, since the change of laser power is a slowly in time varying function. It should be

noted that this uncertainty is a linear function of the intensity of the light incident on the detector.

In order to minimize the influence of lighting conditions on the quality of the signal measured by the detector, the tests were performed in a shaded room with artificial light sources switched off.

Taking into account the above factors affecting the quality of the detector signal, the relative uncertainty of the sample deformation measurement shall not exceed 0.09%.

For samples with a length of 5 mm, this uncertainty is only 4.5 μm ($R^2 = 0.9998$), whereas the uncertainty in determining the slope coefficients of the calibration lines has the greatest impact on this value. For example, if R^2 parameter for the slope coefficients of the calibration lines is equal to 1, the measurement uncertainty of the length shall be about 300 nm.

Further reduction of the measurement uncertainty may occur only through application of optoelectronic devices characterized by very low own noise, high power stability and uniformity of the laser beam.

4. Results and discussion

In order to assess the accuracy of measurement of the optical extensometer, there was carried out a comparative analysis of the strain amount calculated using two methods: 1-wave analysis (Kolsky method) and a method based on the measurement results of the optical extensometer. The maximum strain values calculated using the above methods were determined and designated: ϵ_{wave} , ϵ_{opto} , respectively; they are presented in Table 1. In addition, Table 1 shows the difference between the maximum

Table 1
Comparison of strain ϵ_{opto} and ϵ_{wave} determined for specimens made of different materials (Al 5251, Cu OFE)

test	ϵ_{wave}	ϵ_{opto}	$\epsilon_{wave} - \epsilon_{opto}$
Al 5251			
1	0.21283	0.20120	0.01163
2	0.20453	0.19640	0.00813
3	0.17797	0.16500	0.01297
4	0.16007	0.15050	0.00957
Cu OFE			
1	0.14120	0.12620	0.015
2	0.11010	0.09720	0.0129
3	0.23883	0.20450	0.03433
4	0.22299	0.19090	0.03209

strain determined from measurements carried out using the optical extensometer and the Kolsky method.

The smallest difference occurred in the case of the material with the lowest density, i.e., 5251 aluminum (average difference value 0.0106). It should be emphasized here that the maximum

strain measured with the non-contact method was lower than that obtained using the Kolsky method.

Comparison of the strain history for the specimens made of the tested materials (Fig. 6) provide additional information about the differences in the values of strain for samples calculated on the basis of data obtained with the above-mentioned methods. In all the considered cases of specimens materials, in the initial phase of strain measurement, there occurs a great compliance between the results obtained with the 1-wave analysis and the optical extensometer (strain equal to approximately 0.02).

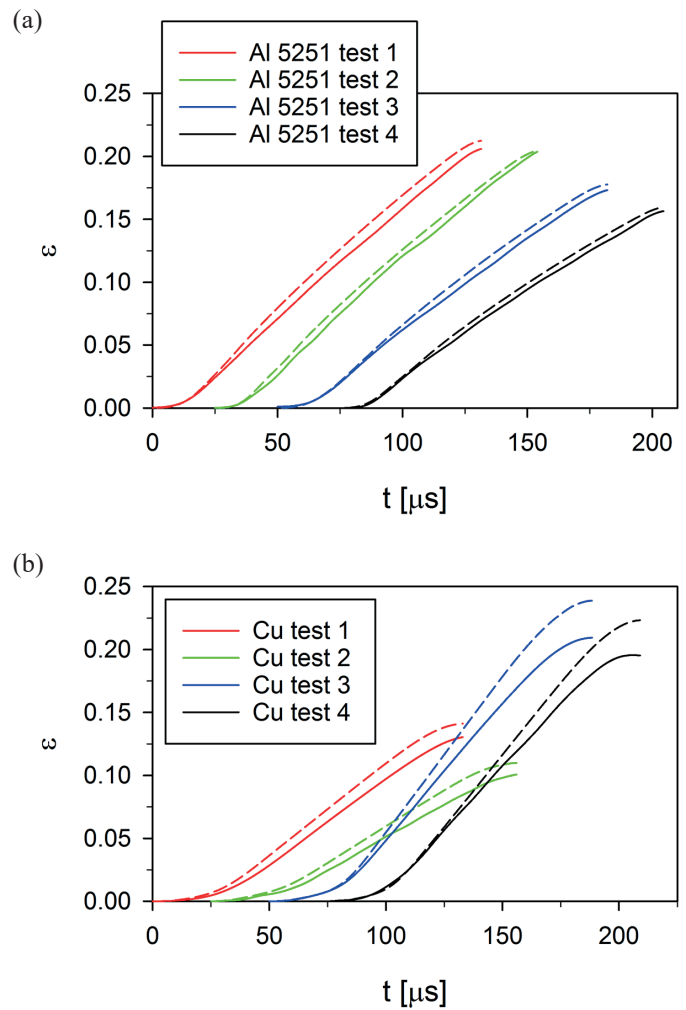


Fig. 6. Comparison of strain history in the specimens obtained from strain gage (dashed lines) and laser extensometer measurements (solid lines): a) Al 5251, b) Cu OFE. The lines were shifted in the increment of 25 ms for ease of comparison

In the case of material with the lowest plastic flow stress, i.e., Al 5251 (Fig. 6a), the differences in the waveforms are relatively small. In Fig. 6b, an additional influence of the strain rate on a difference in waveforms of strain vs. time curves for samples made of Cu OFE can be observed. Curves 1 and 2 were obtained on the basis of the tests performed at the strain rate of

1200 1/s, whereas the strain rates for tests 3 and 4 were equal to approximately 2000 1/s.

The strain vs. time courses differ mainly with a slope angle of curves, which results in differences in the average values of the specimens strain rate. Table 2 compares the average strain rates calculated on the basis of linear approximation of the strain vs. time curve in the range of the most linear characteristic. The calculated values of $\dot{\epsilon}_{wave}$ were greater than $\dot{\epsilon}_{opto}$, however, the greatest differences occurred for tests with the specimens made of Cu OFE which deformed with the highest strain rate.

Table 2

Comparison of strain rates $\dot{\epsilon}_{opto}$, $\dot{\epsilon}_{wave}$ determined for specimens made of different materials (Al 5251, Cu OFE)

test	$\dot{\epsilon}_{wave}$	$\dot{\epsilon}_{opto}$	$\dot{\epsilon}_{wave} - \dot{\epsilon}_{opto}$
Al 5251			
1	1840	1770	-70
2	1730	1740	10
3	1560	1480	-80
4	1350	1310	-40
Cu OFE			
1	1470	1370	-100
2	1160	1050	-110
3	2480	2180	-300
4	2290	2010	-280

The differences in the strain vs. time curves are clearly reflected in the profile of stress vs. strain curves (Fig. 7). The stress vs. strain curves, obtained based on the results from the

laser extensometer in the range of plastic deformation, are above the curves obtained using a 1-wave analysis. These differences are more evident for the higher strain and a higher strain rate. The greatest differences are 7.7 MPa and 20 MPa for Al 5251 and Cu OFE, respectively. The highest compliance of stress vs. strain curves determined with both methods is found for Cu OFE in the case of tests 1 and 2 conducted for a low strain rate (the difference is not greater than 7 MPa).

5. Summary

In the authors' opinion, a splitting-beam laser extensometer technique is an excellent tool for strain measurement of a specimen loaded under Kolsky compression bar experiments. It enables strain measurement with accuracy not less than 0.1%, which corresponds to measurement uncertainty at the level lower than 5 μm . High accuracy of the discussed measurement system was experimentally verified for selected conditions of the experiment, i.e., type of bar materials, specimen materials (Al 5251, Cu OFE) and various strain rates (1100 – 2500 1/s). A comparison of stress-strain curves shows that the level of strains determined with a non-contact method is lower compared to the values determined with 1-wave analysis (strain gauge technique) independently on the assumed conditions of the experiment. The presented non-contact method of the strain measurement can be used in research into porous, soft and low strength materials compared to the strength of the bars materials. The method eliminates the problems associated with noise and low transmitted signal level. It should be noted that in the case of testing the high strength materials, the results obtained with laser extensometer may be encumbered with greater errors due to the punching effect [3, 4].

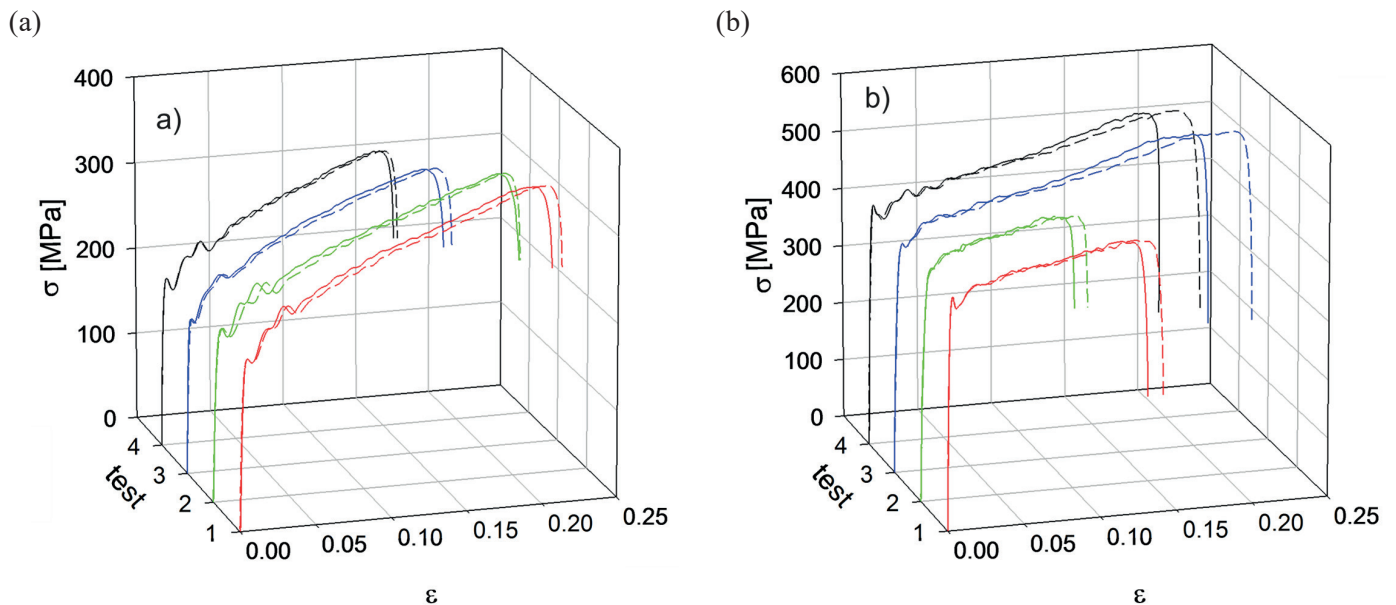


Fig. 7. The engineering compression stress-strain curves from strain gage (dashed lines) and laser extensometer measurements (solid lines) of: a) Al 5251, b) Cu OFE

REFERENCES

- [1] W. Chen, B. Song B, *Split Hopkinson (Kolsky) Bar: Design, Testing and Applications*, Springer, Berlin, 2011.
- [2] A. G. Bazle, J. W. Gillespie, "Numerical Hopkinson bar analysis: uni-axial stress and planar bar-specimen interface conditions by design", *Report MD 21005-5069, ARL-CR-553*, Army Research Laboratory, Aberdeen Proving Ground, 2004.
- [3] K. Safa, G. Gary, "Displacement correction for punching at a dynamically loaded bar end", *Int. J. Impact Eng.* 37, 371-384 (2010).
- [4] T. Jankowiak, A. Rusinek, T. Łodygowski, "Validation of the Klepaczko-Malinowski model for friction correction and recommendations on split Hopkinson pressure bar", *Finite Elements in Analysis and Design* 47 (10), 1191-1208 (2011).
- [5] B. Song, K. Nelson, R. Lipinski, J. Bignell, G. Ulrich, E. P. George, "Dynamic high-temperature testing of an iridium alloy in compression at high-strain rates", *Strain* 50 (6), 539-546 (2014).
- [6] R. Panowicz, J. Janiszewski, "Tensile split Hopkinson bar technique: numerical analysis on the problem of wave disturbance and specimen geometry selection", *Metrology and Measurement Systems* 23 (3), 425-436 (2016).
- [7] K. Xia, W. Yao, "Dynamic rock tests using split Hopkinson (Kolsky) bar system - a review", *Journal of Rock Mechanics and Geotechnical Engineering* 7, 27-59 (2015).
- [8] B. Song, B. R. Antoun, H. Jin, "Dynamic tensile characterization of a 4330-V steel with Kolsky bar techniques", *Experimental Mechanics* 53, 1519-1529 (2013).
- [9] X. Wu, D. A. Gorham, "Stress equilibrium in the split Hopkinson pressure bar test", *Journal de Physique IV Colloque 07 (C3)*, 91-96 (1997).
- [10] D. A. Gorham, "Measurement of stress-strain properties of strong metals at very high strain rates", *Inst. Phys. Conf. Ser.* 47, 16-24 (1980).
- [11] D. A. Gorham, P. H. Pope, J. E. Field, "An improved method for compressive stress-strain measurements at very high strain rates", *Proc. R. Soc. Lond. A* 438, 153-170 (1992), doi: 10.1098/rspa.1992.0099.
- [12] C. C. Roth, G. Gary, D. Mohr, "Compact SHPB system for intermediate and high strain rate plasticity and fracture testing of sheet metal", *Experimental Mechanics* 55 (9), 1803-1811 (2015).
- [13] J. J. Chen, B. Q. Guo, H. B. Liu, H. Liu, P. W. Chen, "Dynamic Brazilian test of brittle materials using the split Hopkinson pressure bar and digital image correlation", *Strain* 50, 563-570 (2014), doi: 10.1016/j.polymertesting.2014.03.014.
- [14] L. Zhang, T. Wang, Z. Jiang, Q. Kemaoy, Y. Liu, Z. Liu, L. Tang, S. Dong, "High accuracy digital image correlation powered by GPU-based parallel computing", *Optics and Lasers in Engineering* 69, 7-12 (2015), doi: 10.1111/str.12118.
- [15] H. Jin, C. Sciammarella, S. Yoshida, L. Lamberti, *Advancement of Optical Methods in Experimental Mechanics*, vol. 3, Springer, New York, 2014, doi: 10.1007/978-3-319-00768-7.
- [16] W. N. Sharpe, K. G. Hoge, "Specimen strain measurement in the split-Hopkinson-pressure-bar experiment", *Experimental Mechanics* 12 (12), 570-574 (1972).
- [17] D. T. Casem, S. E. Grunschel, B. E. Schuster, "Normal and transverse displacement interferometers applied to small diameter Kolsky bars", *Experimental Mechanics* 52, 173-184 (2012), doi: 10.1007/s11340-011-9524-x
- [18] D. T. Casem, S. E. Grunschel, B. E. Schuster, "Interferometric measurement techniques for small diameter Kolsky bars", *Proc. of the 2010 SEM Annual Conference and Exposition on Experimental and Applied Mechanics*, 973-977, Indianapolis (2010).
- [19] K. T. Ramesh, S. Narasimhan, "Finite deformations and the dynamic measurement of radial strains in compression Kolsky bar experiments", *Int. J. Solids Struct.* 33 (25), 3723-3738 (1996).
- [20] Y. Li, K. Ramesh, "An optical technique for measurement of material properties in the tension Kolsky bar", *Int. J. Impact Eng.* 34, 784-798 (2007).
- [21] X. Nie, B. Song, C. M. Loeffle, "A novel splitting-beam laser extensometer technique for Kolsky tension bar experiment", *J. Dynamic Behavior Mater.* 1, 70-74 (2015), doi: 10.1007/s40870-015-0005-7
- [22] S. Ellwood, L. J. Griffiths, D. J. Parry, "Materials testing at high constant strain rates", *J. Phys. E: Sci. Instrum.* 15: 280-282 (1982).
- [23] C. E. Franz, P. S. Follansbee, W. J. Wright, "New experimental techniques with the split Hopkinson pressure bar", *The 8th International Conference on High Energy Rate Fabrication, Pressure Vessel and Piping Division*, San Antonio (1984).
- [24] B. Song, P. E. Wakeland, M. Furnish, "Dynamic tensile characterization of Vascomax maraging C250 and C300 alloys", *J. Dynamic Behavior Mater.* 1, 153-161 (2015), doi: 10.1007/s40870-015-0016-4
- [25] W. Močko, "Analysis of the impact of the frequency range of the tensometer bridge and projectile geometry on the results of measurements by the split Hopkinson pressure bar method", *Metrology and Measurement Systems* 20 (4), 555-564 (2013).
- [26] *PDA36A (-EC) Si Switchable Gain Detector; User Guide*, Thor-Labs, www.thorlabs.com, accessed 11 June 2016.